

Detailed comparison of Xenon APPI (9.6/8.4 eV), Krypton APPI (10.6/10.0 eV), APCI, and APLI (266 nm) for gas chromatography high resolution mass spectrometry of standards and complex mixtures

Anika Neumann^{1,2#}, Ole Tiemann^{1,2#}, Helly J. Hansen^{1,2}, Christopher P. Ruger^{1,2*}, and Ralf Zimmermann^{1,2,3}

1 – Joint Mass Spectrometry Centre / Chair of Analytical Chemistry, University of Rostock, 18059 Rostock, Germany

2 – Department Life, Light & Matter (LLM), University of Rostock, 18059 Rostock, Germany

3 – Joint Mass Spectrometry Centre, Cooperation Group “Comprehensive Molecular Analytics” (CMA), Helmholtz Zentrum Munchen, Gmunder Strae 37, Munchen, 81479, Germany

* – corresponding author: christopher.rueger@uni-rostock.de

- both authors contributed equally to the manuscript

ORCID

Anika Neumann: 0000-0001-7256-3716

Ole Tiemann: 0000-0002-0872-2732

Ralf Zimmermann: 0000-0002-6280-3218

Christopher P. Ruger: 0000-0001-9634-9239

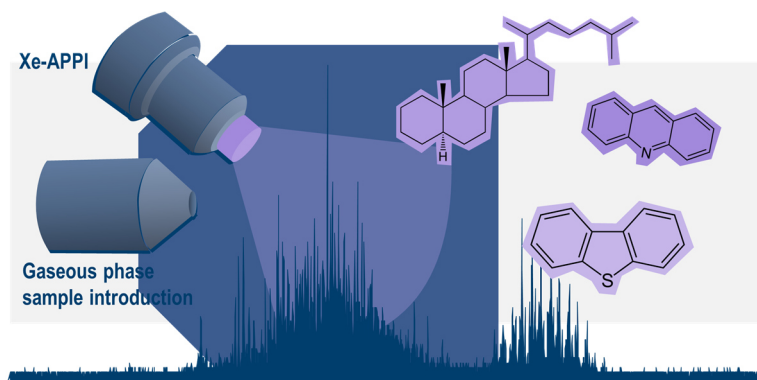
Keywords

mass spectrometry, atmospheric pressure ionisation, photoionisation, polycyclic aromatic hydrocarbons, gas chromatography

Abstract

Photoionisation schemes for mass spectrometry, either by laser or discharge lamps, have been widely examined and deployed. In this work, the ionisation characteristics of a Xenon discharge lamp (Xe-APPI, 9.6/8.4 eV) have been studied and compared to established ionisation schemes, such as atmospheric pressure chemical ionisation, atmospheric pressure photoionisation with a Krypton discharge lamp (Kr-APPI, 10.6/10 eV) and atmospheric pressure laser ionisation (266 nm). Addressing the gas-phase ionisation behaviour has been realised by gas chromatography coupling to high-resolution mass spectrometry without the usage of a dopant. For the multicomponent standard, it has been found that Xe-APPI is able to ionise a broad range of polycyclic aromatic hydrocarbons as well as their heteroatom-containing and alkylated derivatives. However, thiol and ester compounds could not be detected. Moreover, Xe-APPI revealed a high tendency to generate oxygenated artefact, most likely due to a VUV absorption band of oxygen at 148 nm. Beneficially, almost no chemical background, commonly caused by APCI or Kr-APPI due to column bleed, plasticisers or impurities, is observed. This advantage is noteworthy for evolved gas analysis without pre-separation or for chromatographic co-elution. For the complex mixtures, Xe-APPI revealed the predominant generation of radical cations via direct photoionisation with a high selectivity towards aromatic core structures with low alkylation. Interestingly, both Xe-APPI and Kr-APPI could sensitively detect sterane cycloalkanes, validated by gas chromatographic retention. The narrowly ionised chemical space could let Xe-APPI find niche applications, *e.g.*, for strongly contaminated samples to reduce the background.

Table of Content

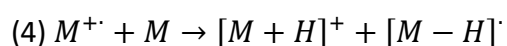
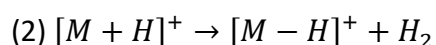
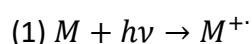


Introduction

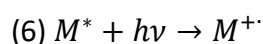
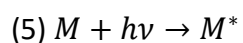
Nowadays, mass spectrometry (MS) is one of the most widely used analytical techniques, classically equipped with electron ionisation (EI).¹ However, over the last decades, advancements in source and ionisation design strongly increased the importance of atmospheric pressure ionisation (API) in mass spectrometry-based analysis.^{2,3,4} Electrospray ionisation (ESI), desorption ionisation techniques, atmospheric pressure chemical ionisation (APCI), atmospheric pressure photoionisation (APPI), and atmospheric pressure laser ionisation (APLI) are well-established techniques in a broad variety of application fields, such as environmental applications, drug and pharmaceutical analysis, life sciences, or petroleomics.^{2,4,5} Developments on API techniques are still ongoing⁶ and novel methods, such as plasma ionisation based on dielectric barrier discharge ionisation (DBDI)⁷ or low-temperature plasma (LTP)⁸, soft X-ray-based APPI⁹, and atmospheric pressure single photon laser ionisation (APSPLI)¹⁰, were recently introduced.

In contrast to EI, which enables universal ionisation, API techniques offer selectivity and sensitivity against specific compound classes. Furthermore, ions do not undergo intensive fragmentation as known from EI but form molecular cations ($M^{+\bullet}$) or quasi-molecular protonated ions $[M+H]^+$. Both of these aspects are especially of interest in complex mixture analysis or target analysis of specific compound classes. In this manuscript, we focus on gas phase ionisation for which API techniques rely on chemical ionisation pathways by ion-molecule reactions or direct photoionisation by the uptake of one or multiple photons.¹¹ The following presented ionisation mechanisms are with special regard to pathways occurring in the gas phase.

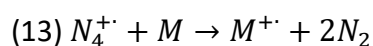
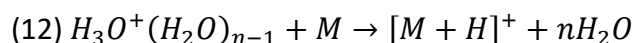
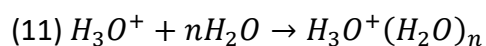
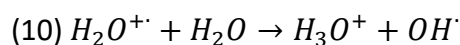
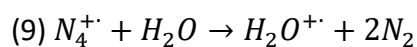
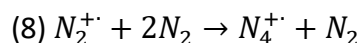
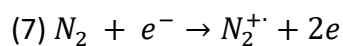
In direct photoionisation, as in APPI, the analyte is ionised by the uptake of one VUV-photon that leads to the formation of a radical cation (1). Thus, all analytes with ionisation potentials below the photon energy can be ionised, including a wide variety of organic compounds, but avoiding the ionisation of common air constituents.¹² Typically, krypton discharge lamps (10.0/10.6 eV) are applied for APPI, but also a rare number of studies investigate other photon energies, such as 8.4 eV (Xenon)¹³, 9.8 eV¹⁴, or 11.7 eV (Argon)¹³. Besides the formation of radical cations, also protonated ions are observed that are formed by proton transfer from a solvent/dopant or ion-molecule reactions between the analytes (2-4) in complex mixtures.^{15,16} Syage et al.¹⁷ investigated the protonation mechanism in detail and reported that protonated ions are formed by a radical cation abstracting a hydrogen atom from a protic solvent (or another analyte).



APLI is based on a resonance-enhanced multiphoton process (typically [1+1]), where the first photon excites the molecule to an intermediate state (5), while the second photon leads to ionisation and formation of a radical cation (6).^{18,19} However, only compounds with an appropriately long lifetime of the excited state, such as polycyclic aromatic hydrocarbons (PAHs), can be ionised by the two-photon process leading to a high selectivity of the method.^{20,21,22} Commonly, Nd:YAG lasers with 266 nm (4.66 eV) and krypton fluoride excimer lasers with 248 nm (5.0 eV) are applied in APLI ionisation.^{19,22,23}



Ionisation in APCI is induced by corona discharge, where primary radical cations are formed by the makeup gas that is commonly nitrogen (7-8). The primary ions then react with traces of water in the ion source and form charged water clusters (9-11). These clusters, in turn, ionise the analytes by proton transfer reactions (12). Nonetheless, also a charge transfer can occur if the ionisation potential of the analyte is below that of N₄ clusters (13).^{4,24}



The way of sample introduction, either in solution or as gaseous phase, has an influence on the ionisation pathway. In liquid introduction, the solvent type or sample matrix can affect the ionisation process by intermolecular interactions.^{25,26} Solvents, which act as dopant can increase a method's sensitivity²⁷, whereas in other cases, the solvent or the sample matrix decrease the intensity or even completely suppress the ionisation of certain analytes.^{14,28} For photon-based API techniques, light absorption by solvent molecules as well as the solvent flow rate plays a role in sensitivity aspects.^{25,29} Gaseous sample introduction by spatial separation of the vaporisation and ionisation process, for example, by gas chromatography (GC)^{30,31} or ion mobility spectrometry (IMS)³², can reduce ion molecule-reactions or solvent/matrix effects. Nonetheless, despite of the separation, both ion types are typically present especially in complex mixtures, where coeluted analytes might interact with each other.

High resolution (HR) Fourier transform ion cyclotron resonance mass spectrometry (FT-ICR MS) has unbeaten mass resolving power and mass accuracy that enables the calculation of sum formulae directly from the detected mass-to-charge (m/z) ratio.³³ In combination with API techniques that produce predominantly molecular ions, thousands of species can be attributed in a single spectrum.³⁴ These outstanding properties allow furthermore for the clear differentiation between protonated ions and radical cations not only for individual standard substances but also in complex mixtures. There is a number of studies that compare different ionisation methods with regard to the addressed compositional space in complex mixtures and preferred ionisation pathways. Crude oil and other petroleum-derived materials as well as new generation bio-oils are often applied for the comparison of ionisation

techniques in combination with HRMS, as they cover a broad compositional space including a broad range of chemical classes.³⁵ A variety of investigations were made on the comparison of direct infusion sample introduction with commercially available API techniques^{36,37,38}, but there is limited research on effects occurring for gaseous phase introduction. Nonetheless, several standard compounds were investigated by Kauppila et al. concerning ion type formation and chemical coverage of APPI and APLI with and without dopant using gaseous phase introduction by GC-HRMS.¹⁹

In this study, we explore Xenon-based APPI (Xe-APPI, 9.6/8.4 eV) as ionisation technique for GC-HRMS in comparison to classical Kr-APPI (10.6/10 eV), APLI (266 nm, 4.7 eV) and APCI (Corona discharge electrode). Therefore, multiple standard compounds, including PAHs, heteroatom-containing PAHs, steranes, and esters, were investigated. Furthermore, also the influence of proton and charge transfer reactions in complex mixtures is addressed by the investigation of exemplary petroleum-derived samples. We focus especially on ionisation efficiency, the type of the formed ions (protonated or radical cation), fragmentation of the analytes, and the formation of ionisation artifacts by reaction with oxygen. Furthermore, also the influence of proton and charge transfer reactions in complex mixtures is addressed by the investigation of exemplary petroleum-derived samples.

Methods and Materials

Standard Solutions and Complex Mixtures

EPA PAH 525 Mix A was purchased from Sigma Aldrich. M1 standard solution is a self-made standard solution holding 17 alkylated PAHs and three sulphur containing aromatics diluted in toluene. Mix 2 includes several heteroatom containing aromatics, as well as fatty acid and 5- α -Cholestane diluted in toluene. Detailed information about M1 and Mix 2 standard solutions are shown in the supporting information (Table S1/S2). For GC FT-ICR MS, the standard stock solutions were diluted in dichloromethane (LiChrosolv, Supelco, Merck KGaA, Darmstadt, Germany) with a final concentration for each compound of 1 to 5 mg/L.

Gas Chromatography coupled with Atmospheric Pressure Ionisation Fourier Transform Ion Cyclotron Resonance Mass Spectrometry (GC-APXI-FT-ICR MS).

Each standard solution and complex mixture was analysed separately. For the analysis, the dissolved and diluted sample was introduced in a microliter vial (Agilent Technologies, Santa Clara, USA) to the programmable temperature vaporiser (PTV) injector (1079 Universal Capillary Injector with a large volume adapter, Varian Inc., Palo Alto, USA). For the separation, a 30 m Rxi-5HT column with 320 μ m inner diameter and a 0.1 μ m film thickness was implemented and helium was used as carrier gas with a linear velocity of 1 mL/min. The temperature programs for both, the PTV injector and the GC oven are shown in Table 1.

Table 1. Temperature programs of the PTV injector and the GC oven for the standard solutions, lower distillation cuts and higher distillation cuts.

	PTV injector	GC oven	
		Low cut*	High cut**
Initial temperature (hold time)	50°C (1 min)	50°C (5 min)	50°C (5 min)
Heating rate	150°C/min	5°C/min	5°C/min
Final temperature (hold time)	300°C (5 min)	300°C (0 min)	320°C (10 min)

*Low cut includes all lower distillation cuts such as B0_W, H0_1, MGO, and the CPC blend cuts from 200°C to 320°C, as well as the standard solutions., **High cut includes the higher distillation cuts such as HFO, the CPC Blend and the CPC blend cuts from 320°C to 380°C.

After separation, the compounds were transferred to a modified GC-APCI II source (Bruker Daltonics, Bremen, Germany) via a self-built transferline, which was heated at 250 °C. Ionisation was done with two different types of atmospheric pressure photoionisation (APPI), atmospheric pressure chemical ionisation (APCI) and atmospheric pressure laser ionisation (APLI). For APPI, a Krypton lamp (APPI-Kr) and a Xenon lamp (APPI-Xe) were used with a photon energy of 10.0/10.6 eV and 8.4 eV, respectively. APCI was operated with a needle current of 3000 nA and for APLI a NdYAG-laser with a wavelength of 266 nm and a laser energy of 3 mJ/cm² was utilized. To suppress contamination inside the ion source, the nebuliser gas stream was set to 3 L/min and dry gas stream was set to 2 L/min for APPI and APLI and to 6 L/min and 1 L/min for APCI, respectively. The EPA PAH 525 Mix A solution was measured every day for performance control.

The time-resolved mass spectra were recorded on a 7 T Fourier transform ion cyclotron resonance mass spectrometer (APEX Qe, Bruker Daltonics, Bremen, Germany). A 1 s transient (2 Megaword) lead to a resolution of 150,000 @ m/z 400. Precalibration and pretreatment of the measurements were carried out in Data Analysis 5.1 (Bruker Daltonics, Bremen, Germany). Ion chromatograms of the standard compounds were extracted and integrated by Visual Basic scripting. Further data treatment of the complex samples was performed in CERES, a self-written program based on MATLAB scripting (MATLAB R2020b). Details are given elsewhere.^{30,39} Mass spectra were linearly recalibrated scan by scan on internal homologues rows and, subsequently, blank corrected with an external background list containing interferences such as source background and impurities found in the GC run as well as column bleed. Sum formula assignment was carried out with the following restrictions: #C 4-100, #H 4-200, #N 0-1, #O 0-4, #S 0-1, mass error ± 1 ppm.

Results and Discussion

Standard compounds

Compositional coverage by Xe-APPI, Kr-APPI, APLI and APCI for standard substances

The three main atmospheric pressure ionisation sources for gas-phase ionisation, namely Kr-APPI, APLI, and APCI, were utilised to analyse standard substances and were compared to rarely used Xe-APPI. Table 2 shows all substances contained in the standard mixtures and whether or not they were ionised by the utilised techniques. Most of the investigated compounds were ionisable throughout all ionisation techniques. According to the literature, Kr-APPI is considered an almost universal ionisation method^{16,40,41}, suitable to ionise all compounds with an ionisation energy below 10.0 eV. As a result, all compounds included in the standard solution were ionised by Kr-APPI. Polycyclic aromatic hydrocarbons were ionised by all ionisation techniques regardless of the size of aromatic core or the grade of alkylation. However, acenaphthylene was the only exception not being detectable by APLI due to the short lifetime (picosecond time scale) of the first excited state and its low absorption of radiation at 266 nm.^{42,43} While alkylation does not influence the ionisability (e.g., pyrene, 1-methylpyrene, 1-ethylpyrene), the addition of a thiol-group shows influences on the detection (e.g., 2-methylnaphthalene, 2-naphthalenethiol) in Xe-APPI, APLI and APCI. Huba et al. stated that pure alkanes without any functionalisation can only be ionised by direct infusion API under very specific conditions.³⁸ By analysing a sterane derivative and a fatty acid ester, it was found that Kr-APPI and APCI were capable to ionise both compounds, while Xe-APPI only ionised 5- α -cholestane. Thus, although steranes are saturated non-functionalised hydrocarbons, they are ionisable by several techniques. APLI could ionise neither steranes nor carboxylic esters. In addition, also benzothiophene and acridine were not ionisable, while dibenzothiophene and carbazole were ionised by APLI. Furthermore, the direct comparison of Kr-APPI and Xe-APPI showed that, although both techniques ionised a very similar chemical range, the detected abundances for Xe-APPI were significantly lower than for Kr-APPI across all compounds.

Table 2. Ionisation of analytical standard compounds by Xe-APPI, Kr-APPI, APLI and APCI grouped according to their compound classes and functionalities. Compounds with a signal-to-noise ratio larger than six for their molecular $[M]^{+•}$ or quasi-molecular $[M+H]^+$ peak were depicted with a checkmark.

			Xe-APPI	Kr-APPI	APLI	APCI
Polycyclic aromatic hydrocarbons	PAH cores	Acenaphthylene	✓	✓	-	✓
		Fluorene	✓	✓	✓	✓
		Phenanthrene	✓	✓	✓	✓
		Anthracene	✓	✓	✓	✓
		Pyrene	✓	✓	✓	✓
		Benz[a]anthracene	✓	✓	✓	✓
		Chrysene	✓	✓	✓	✓
		Benzo[b]fluoranthene	✓	✓	✓	✓
		Benzo[k]fluoranthene	✓	✓	✓	✓
		Benzo[a]pyrene	✓	✓	✓	✓
		Indeno[1,2,3-c,d]pyrene	✓	✓	✓	✓
		Dibenz[a,h]anthracene	✓	✓	✓	✓
		Benzo[g,h,i]perylene	✓	✓	✓	✓
		Coronene	✓	✓	✓	✓
	Alkylated PAHs	2-Methylnaphthalene	✓	✓	✓	✓
		1,2-Dimethylnaphthalene	✓	✓	✓	✓
		1,3,7-Trimethylnaphthalene	✓	✓	✓	✓
		3-Methylfluorene	✓	✓	✓	✓
		1-Methylfluorene	✓	✓	✓	✓
		9-Methylphenanthrene	✓	✓	✓	✓
		3-Methylphenanthrene	✓	✓	✓	✓
		3,6-Dimethylphenanthrene	✓	✓	✓	✓
		9,10-Dimethylphenanthrene	✓	✓	✓	✓
		Retene	✓	✓	✓	✓
		1,2,4-Trimethylantracene	✓	✓	✓	✓
		2,3,6,7-Tetramethylantracene	✓	✓	✓	✓
		1-Methylpyrene	✓	✓	✓	✓
		4,5-Dimethylpyrene	✓	✓	✓	✓
		1,3,6,8-Tetramethylpyrene	✓	✓	✓	✓
		1-Methylbenz[a]anthracene	✓	✓	✓	✓
		7,12-Dimethylbenz[a]anthracene	✓	✓	✓	✓
		1-Ethylpyrene	✓	✓	✓	✓
		6-Ethylchrysene	✓	✓	✓	✓
PAH-Thiol		2-Naphthalenethiol	-	✓	-	-
Sulphur PAHs	S-PAH cores	Benzo[thiophene]	✓	✓	-	✓
		Dibenzo[thiophene]	✓	✓	✓	✓
		Benzo[b]naphtho[2,1-d]thiophene	✓	✓	✓	✓
		Benzo[b]naphtho[1,2-d]thiophene	✓	✓	✓	✓
		Naphtho[1,2-b:5,6-b']dithiophene	✓	✓	✓	✓
	Alkylated S-PAH	4,6-Diethyldibenzo[thiophene]	✓	✓	✓	✓
	N-PAH cores	Carbazole	✓	✓	✓	✓
		Acridine	✓	✓	-	✓
Alkylated N-PAH	3-Ethylcarbazole	✓	✓	✓	✓	
Steran		5- α -Cholestane	✓	✓	-	✓
Ester		Methylpalmitate	-	✓	-	✓

Influence of chemical class, alkylation and aromatic ring-size on the formation of radical cations and protonated ions

For insight into the structural-dependant ionisation behaviour, Figure 1 visualises the intensities of selected components normalised to their injection concentration. While Xe-APPI, Kr-APPI and APLI almost exclusively generate odd ions, APCI preferably forms even ions while simultaneously producing a certain degree of odd ions. With increasing ring size, the formation of even quasimolecular ions also increases slightly (Figure S1/S2).

For APCI, the odd/even-ratio depends strongly on the compound class. Methyl palmitate, for example, was found to be preferentially ionised forming $[M+H]^+$ ions, as the polar carbonylic functional group favours protonation. Sulphur-containing PAH (S-PAH) cores revealed that the average odd/even-ratio is higher than the average odd/even ratio for homoatomic PAH cores. On the other hand, for nitrogen-containing PAH (N-PAH) cores, lower odd/even ratios were found (Table S3). Furthermore, an increasing ring size leads to enhanced protonation in APCI, which agrees with the results from literature-reported direct infusion experiments.³⁸ Additionally, alkylation reduced the odd/even ratios leading to the assumption that alkylation increases proton affinity. However, it was noted, that the type of alkylation (*e.g.*, methylation, dimethylation, ethylation) showed no significant influence on the ionisation behaviour by APCI (*e.g.*, pyrene: odd/even = 0.34, 1-methylpyrene: odd/even = 0.11, 1-ethylpyrene: odd/even = 0.10, 4,5-dimethylpyrene: odd/even = 0.11). Furthermore, for alkylated compounds, the odd/even ratios were found to show no significant differences between PAHs (0.137 ± 0.022), N-PAHs (0.123) and S-PAHs (0.115). The averaged odd/even ratios of the alkylated compounds are found to be lower than the ratios of their core structures, regardless of the heteroatom.

For all techniques, it was observed that alkylation led to an increased intensity compared to the corresponding non-alkylated cores. This effect was rather small for both APPI techniques and APCI, while being very pronounced for APLI. It was also found that isomers showed significant differences in their ionisation efficiency by APLI, while almost no influence was detected for APPI and APCI. According to Heafliiger and Zenobi⁴³, isomers have different lifetimes of the first excited state and show different levels of absorption at 266 nm, resulting in differing ionisation efficiencies, mostly causing the described observations.

As shown in Table 1, 5- α -cholestane was ionised by Xe-APPI, Kr-APPI and APCI. Interestingly, the molecular ion was almost exclusively detected as radical cation. However, by comparing the abundances of 5- α -cholestane between the API techniques, the abundances by Xe-APPI and APCI are rather low, whereas Kr-APPI shows a higher sensitivity towards this sterane derivative than towards non-alkylated S- and N-PAHs. Since both, (poly-)aromatic and polycyclic hydrocarbons are ionised by Xe-APPI, Kr-APPI and APCI, (poly-)aromatic and polycyclic compounds with identical sum formulae can only be distinguished with high confidence by APLI, as saturated polycyclic compounds cannot be ionised with this technique.

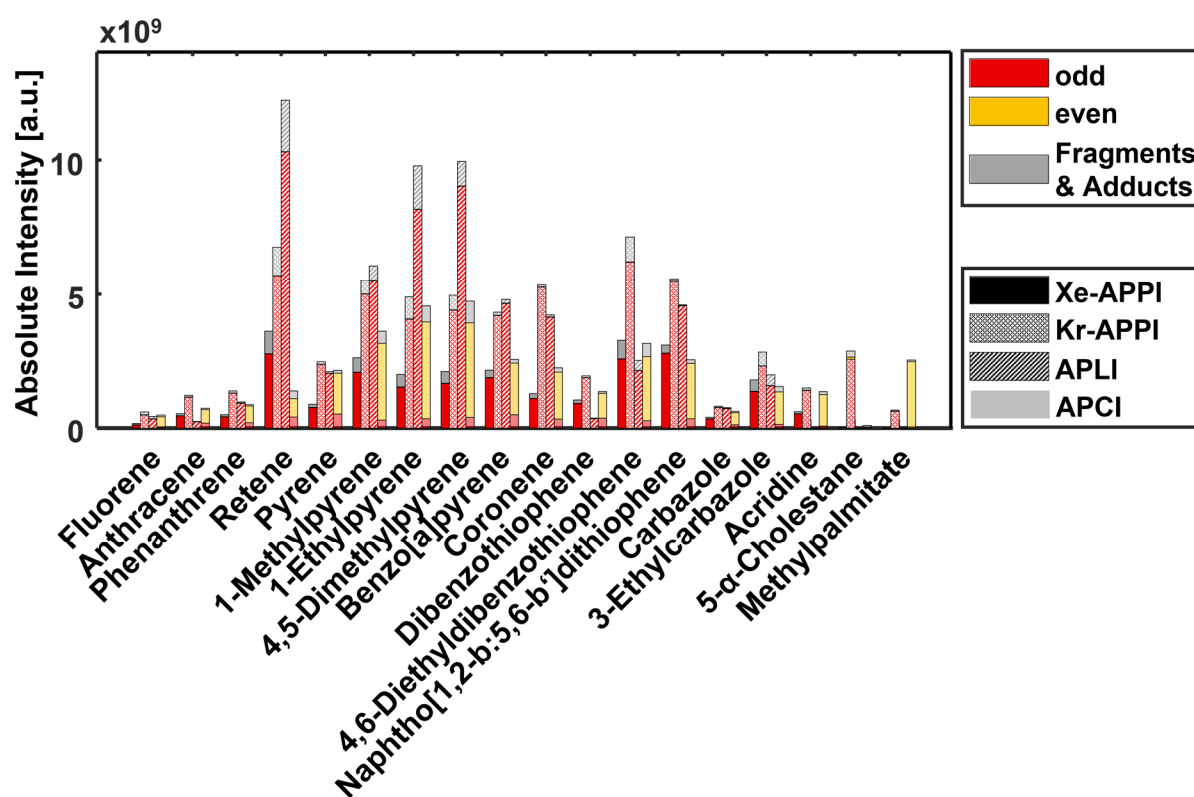


Figure 1. Stacked bar plot visualising the intensity of (quasi-)molecular ions with odd and even electron configuration as well as the summed intensity of fragments and adducts (colour-coded). For each group, the bars are assigned to the ionisation techniques as follows: Xe-APPI (full body), Kr-APPI (dotted), APLI (striped), APCI (partially opaque). The intensities were normalised to the injected concentrations.

Fragmentation and ionisation artefacts

Details on and the detected fragments and adducts are depicted in Figure 2. For mono-methylated compounds, hydride abstraction was the most common fragmentation across all ionisation techniques. For Xe-APPI, Kr-APPI and APLI ethylated compounds showed preferentially demethylation as fragmentation pathway. Besides demethylation, APCI also showed strong cleavage of C₂H₃-fragments (*e.g.*, 1-ethylpyrene, 4,6-diethyldibenzothiophene). Interestingly, dimethylated compounds mainly showed demethylation leading to [M-CH₃]⁺-fragments. Severe demethylation was observed for compounds in which the methyl groups were attached to adjacent carbon atoms. For compounds with identical aromatic cores, significant hydride abstraction was detected when the methyl groups were not bound to adjacent carbons, while simultaneously demethylation was less intense. This observation agrees with the electron ionisation (EI) mass spectra in the national institute of standards and technology (NIST) database.⁴⁴

Compared to the alkylated PAH compounds, 5- α -cholestane showed rather different fragmentation in both APPI techniques. Strong dealkylation was found with the main fragments being $m/z = 203, 217, 218$ and 262 (Figure S3), which are in agreement with fragments found by electron ionisation. The highest fragment observed for APCI was the hydride abstracted [M-H]⁺ ion.⁴⁵

For Xe-APPI, strong oxygenation was observed with about 10 % of the compound's intensities being oxygenated species. Kersten et al. did mechanistic investigations on the oxidation of pyrene in krypton-based APPI as well as VUV-APLI and found that the addition of a OH radical with subsequent H-abstraction was the main oxidation mechanism.⁴⁶ For pyrene, the 217 ([M+15]⁺) was observed as a main signal, but in the present study, predominantly 218 ([M+16]⁺) and 219 ([M+17]⁺) were observed as oxidation artefacts. These differences might be caused by different reaction conditions in the ion source. Despite of that, we observed a remarkably higher content of oxidised species for Xe-APPI than for Kr-APPI. Lu et al. found strong absorption of VUV radiation for oxygen around 8.4 eV (147.60 nm), while for 10.0 eV (123.98 nm) and 10.6 eV (116.97 eV) barely any absorption was observed.⁴⁷ Therefore, we hypothesise that the VUV radiation of 8.4 eV leads to the formation of a higher proportion of oxygen radicals and ozone, which in turn can form a higher number of OH-radicals that can react with the analytes.⁴⁶

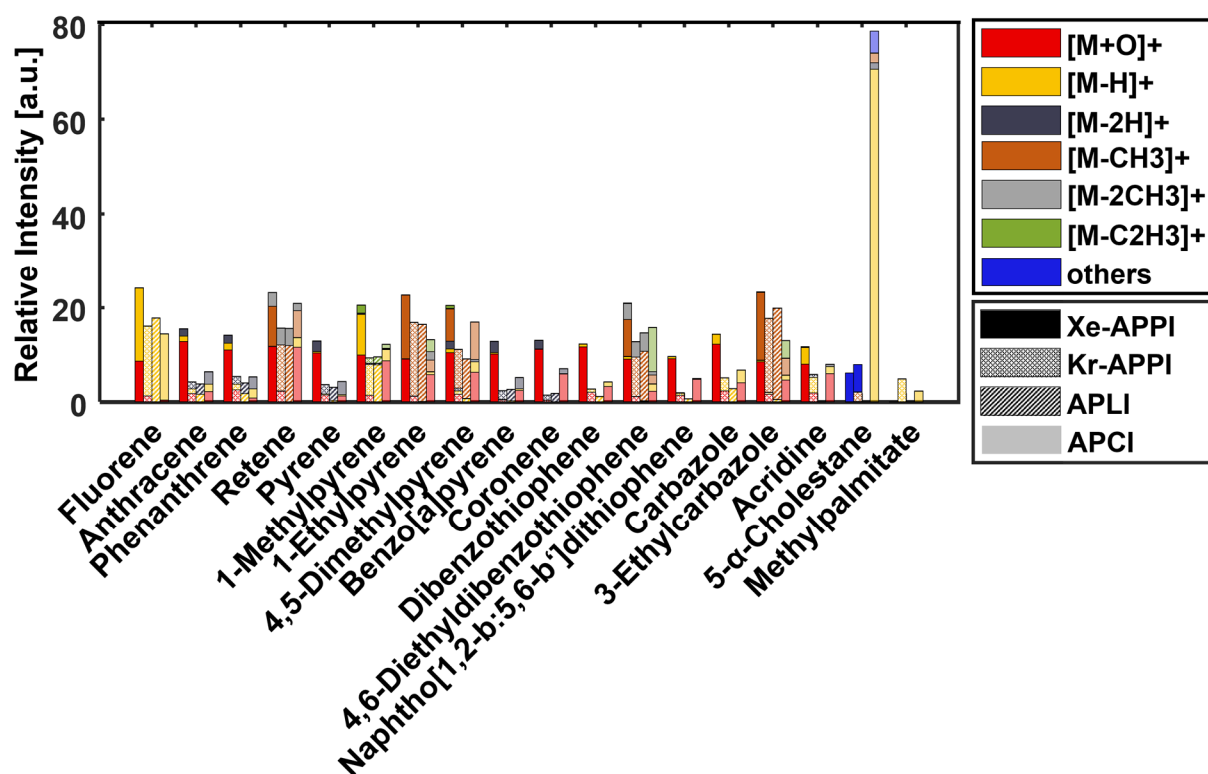


Figure 2. Stacked bar plot visualising the relative contribution of fragment and adduct ions (colour-coded) for selected standard compounds. “Others” includes all fragments showing a higher degree of dealkylation than those listed. For each group, the bars are assigned to the ionisation techniques as follows: Xe-APPI (full body), Kr-APPI (dotted), APLI (striped), APCI (partially opaque). The intensities were normalised to the injected concentrations.

Background

Chemical background in the ion source, impurities from sample preparation, or even the sample matrix can strongly affect the analyte spectrum in terms of ion suppression during the ionisation process. High interference signals have classically almost no impact on the analyte intensity detected by time-of-flight systems or quadrupole mass spectrometers, but linear ion traps and even more FT-devices (FT-ICR MS, Orbitrap) are affected by space charge effects during the measurement. Depending on the research question and application, the choice of the ionisation method could also be driven by the ability to blank out background signals. In Figure 3, the total ion chromatogram (TIC) for gas chromatographic analysis of the pure solvent (dichloromethane) is shown for the four ionisation techniques. Strikingly, Xe-APPI and APLI reveal almost no background signals, whereas the widely applied techniques Kr-APPI and APCI occasionally show high interferences. For both Kr-APPI and APCI, column bleed leads to high background signals at higher GC temperatures. Furthermore, APCI is strongly affected by

fatty acid contamination and plasticisers permanently present as ion source contamination (Figure S4). The low background contamination of Xe-APPI could be of great advantage for samples contaminated with highly polar substances and which cannot be measured with prior GC separation or strong co-elution. In Figure S5 in the supplemental material, we show a highly complex asphaltene sample measured by thermogravimetry coupled to FT-ICR MS^{48,49}, measured with both, Xe-APPI and Kr-APPI. For Kr-APPI, the spectrum is highly dominated by the contaminant signal (most likely a plasticiser), whereas the interference was almost absent with Xe-APPI.

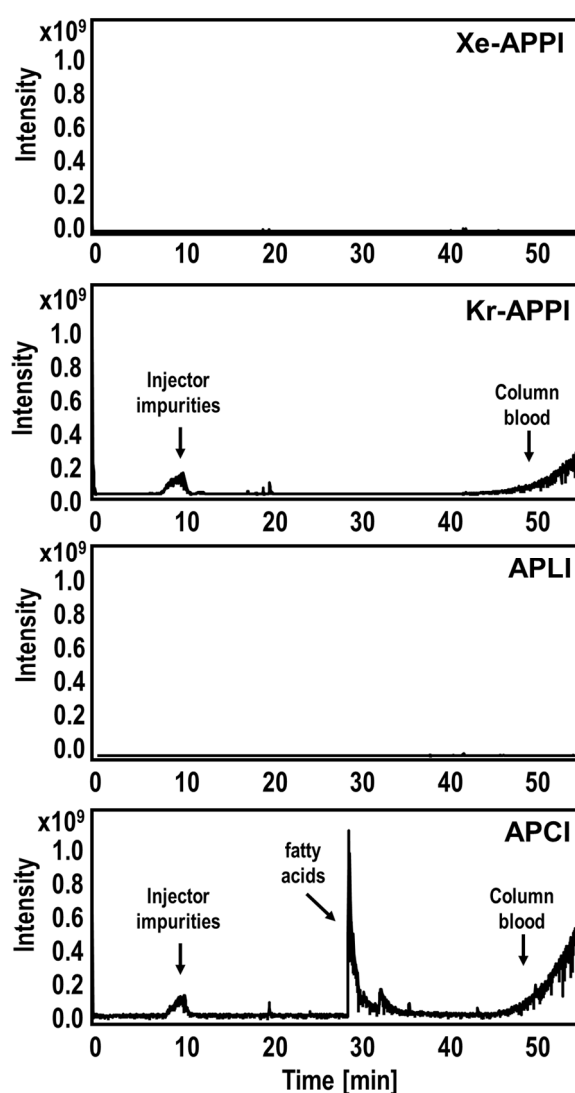


Figure 3. Total ion chromatogram (TIC) of the solvent (dichloromethane) measured by GC-FT-ICR MS compared for all ionisation techniques. Xe-APPI and APLI revealed almost no background signal in the ion source or during the GC measurement. Kr-APPI and APCI were affected by general impurities occurring from the GC set-up as well as the column blood at higher temperatures. APCI further ionises fatty acids and plasticisers present as background signals in the ion source or solvent.

Complex mixtures

The ionisation processes in complex mixtures could differ from the ionisation processes observed for the standard substances due to ion-ion and ion-molecule interaction.³⁸ Because of gas chromatographic co-elution, molecular interactions between different types of analytes occur predominantly, leading to proton or charge transfer reactions.³⁸ However, odd and even electron configuration ions have also been found for the analytical standards. The presence of both of these ion types for one analyte, protonated molecular ions $[M+H]^+$ and radical cations $[M]^{+\bullet}$, clearly complicates the mass spectra, which then requires higher mass resolution or chromatographic separation capabilities to avoid misinterpretation of the data. In the following section, the preferred ion type formation as well as compositional space covered by Xe-APPI is evaluated for different complex petroleum-derived samples and the results are compared to Kr-APPI, APCI and APLI.

Compositional coverage by Xe-APPI, Kr-APPI, APLI and APCI in complex mixtures

A first insight into the compositional coverage is given in Figure 4a, where a marine gas oil (MGO) is compared for all techniques and visualised in an UpSet diagram. The UpSet diagram enables the quantitative analysis of intersections between the different data sets, similar to a Venn diagram⁵⁰ but clearer structured for higher numbers of data sets.⁵¹ In the case of API comparison, the UpSet diagram reveals the unique ions detected by each method, but also common ions detected by two or three techniques as well as the ions detected by all four ionisation methods can be easily represented. In complex mixture analysis, compounds are often grouped into compound classes to facilitate the interpretation of the high number of assigned sum formulae. For example, all compounds, containing only carbon and hydrogen, are grouped into the CH-class, whereas compounds containing additional oxygen are grouped into CHO_x-classes. The intersection size is illustrated as stacked bar graph in the UpSet diagram and divided into the different compound classes, facilitating a more in-depth discussion. On the bottom left side of Figure 4a, the number of different ions detected in MGO for each ionisation technique (set size) is presented. Each of these data sets is already the intersection of three replicates, ensuring a high confidence of the assigned sum formulae. APCI revealed the highest overall number of attributed ions (805), followed by Kr-APPI (624), APLI (419), and Xe-APPI (341). Each method also revealed unique ions only detected by this ionisation technique. APCI detects the highest number of unique ions (470), which belong

mostly to oxygen-containing or other polar to semi-polar compound classes especially ionised by the favoured protonation mechanism. APLI exclusively ionises nitrogen-containing aromatics and CH-class compounds, whereas the Kr-APPI ionisation mechanism favours especially sulphur-containing compounds and different CH-class compounds. Xe-APPI only observes a rare number of unique species, which implies that the addressed compositional space is covered by a combination of the other ionisation methods. A number of 155 sum formulae could be detected by all ionisation techniques. To conclude, the high number of detected compounds and the broad chemical coverage of Kr-APPI and APCI explains their great popularity among the different API techniques. However, also APLI and Xe-APPI have their niche applications, *e.g.*, the improvement in chemical background discussed above.

DBE versus carbon number (#C) diagrams are often used in petroleomics to present the covered compositional space and are classically visualised for a selected compound class.⁵² The DBE is defined as the number of rings and **double bond equivalents** in a molecule and can be calculated from attributed sum formulae: $DBE = 1 + C - \frac{\#H}{2} + \frac{\#N}{2}$. Consequently, the compositional space illustrated in a DBE/#C diagram is spanned by aromaticity/unsaturation and the molecular weight of the attributed compounds. With regard to the investigated petroleum-derived samples, highly aromatic core structures can be found at high DBE values and low #C numbers, whereas compounds with a higher degree of alkylation appear at higher #C numbers.⁴⁸ For most compound classes (except nitrogen-containing classes with odd numbers of nitrogen atoms), radical cations have integer DBE values, whereas protonated/deprotonated ions have half-integer DBE values.

In the DBE/#C diagram in Figure 4b, all CH-class compounds detected in MGO by the four ionisation techniques are overlaid. CH-species ionised by all methods are highlighted in dark grey, whereas species uniquely ionised by Kr-APPI, APLI, and APCI are highlighted in red, yellow, and blue, respectively. Remarkably, Xe-APPI did not show any unique CH-compounds. The CH-compounds detected by all techniques are most likely alkylated aromatics with one to three rings (DBE 4-12). Here, both ion types are observed for core structures with low alkylation, whereas radical cations (integer DBE values) also reveal CH-species with carbon numbers up to 25. APLI (yellow) uniquely ionises small aromatic core structures without/short alkylation as well as species with especially high DBE. Kr-APPI (red) extends the compositional space, especially for species with longer alkylation and non-aromatic CH-compounds (DBE <

4). CH-species exclusively detected by APCI (blue) are throughout protonated ions, which is not surprising regarding the dominating ionisation mechanism.⁴

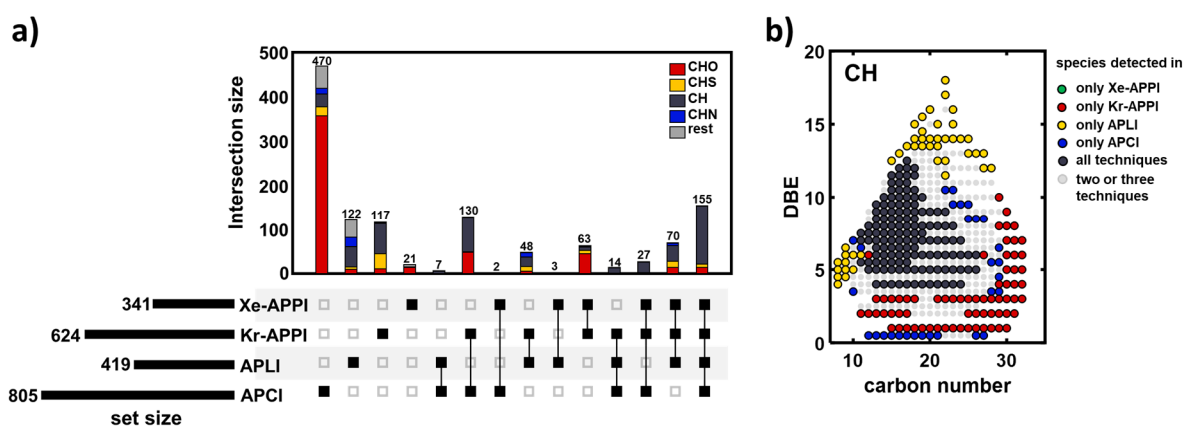


Figure 4. Results of the complex MGO sample. Three replicates are averaged, and only compounds found in all replicates are depicted. a) The UpSet diagram illustrates the uniquely and commonly detected ions of all four ionisation techniques. Each intersection is separated into colour-coded compound classes. b) DBE/#C diagram of the CH-class in MGO overlaid for all ionisation techniques. Common ions are highlighted in dark grey, ions only detected by Kr-APPI, APLI, APCI are highlighted in red, yellow, and blue, respectively.

DBE/#C isoabundance plots shown in Figure 5 illustrate the compositional space addressed by the different ionisation techniques. The respective average abundance is colour-coded. All methods are compared for the CH-class of diesel, MGO and light crude oil. The dashed red line at DBE 4 guides for orientation.

At first glance, differences between the ionisation techniques become apparent that are strongly linked to DBE/aromaticity.³⁷ To be more precise, Xe-APPI predominantly generates radical cations (64-93% of the assigned sum formulae) and is even more shifted into the direction of radical cations as the samples become heavier and more aromatic. The lightest detected CH-compounds have at least a DBE of 4 (one aromatic ring). Furthermore, compared to Kr-APPI, a lower degree of alkylation has been found on average. Xe-APPI especially addresses aromatic core structures (DBE 7-10) with low alkylation (#C < 20). Although both techniques are based on a UV light absorption, the focus of the addressed chemical space by Kr-APPI is remarkably different. These observations might be an effect of prevalent direct photoionisation in Xe-APPI and only minor contribution of proton or charge transfer reactions. Short et al. investigated different wavelength for APPI-LC-MS and found that photons emitted by a Xenon discharge lamp have higher penetration depths into the ion source volume¹³, which might present an explanation for the favoured direct photoionisation

mechanism. In liquid chromatography mass spectrometry, VUV photons can only penetrate less than 5 mm into the ion source volume.⁴⁶ Interestingly, despite the use of GC separation to avoid solvent effects, we observe comparable results in our study.

In contrast to Xe-APPI, Kr-APPI shows high abundances for CH-compounds with lower DBE values of 4 to 6 and longer degree of alkylation and also non-aromatic species with DBEs below 4 can also be ionised by Kr-APPI. Especially in this compositional region, protonated ions occur alongside with radical cations. We assume that here, besides the direct ionisation because of the higher photon energies, chemical ionisation pathways by proton or transfer reactions play a major role in the ionisation mechanism.

APLI covers a remarkably different compositional space compared to all the other ionisation techniques. The detected CH-compounds are clearly shifted toward core aromatic structures with only low alkylation degree and even compounds with higher DBE values than found by the other methods were observed. Interestingly, for particularly high DBE values, also compounds with higher alkylation degree were detected. Benigni et al. compared direct infusion APLI and GC-APLI for the detection of aromatic compounds in petroleum-derived mixtures and found predominantly compounds with smaller m/z values (correlating with lower alkylation) by GC-APLI.²¹ These findings as well as our results suggest that gas phase ionisation APLI especially highlights aromatic core structures that are suppressed in direct infusion sample introduction. Interestingly, in our study, particularly for high DBE values, also compounds with higher alkylation degree were detected. This effect might be explained by the increased ionisation cross section of larger PAHs⁵³, allowing for the detection of the very low abundant alkylated high aromatic compounds.

APCI preferentially produces protonated ions (77-93% of the attributed compounds) and covers a similar compositional space as Kr-APPI for lighter petroleum fractions. However, for the more complex light crude oil, especially CH-compounds with low DBE values were ionised. As APCI is more prone to ionise polar and semipolar compounds, non-polar CH- or and S-class species are presumably suppressed in the presence of preferentially ionised compounds. This observation points towards matrix effects because of chromatographic co-elution in the high complex samples.

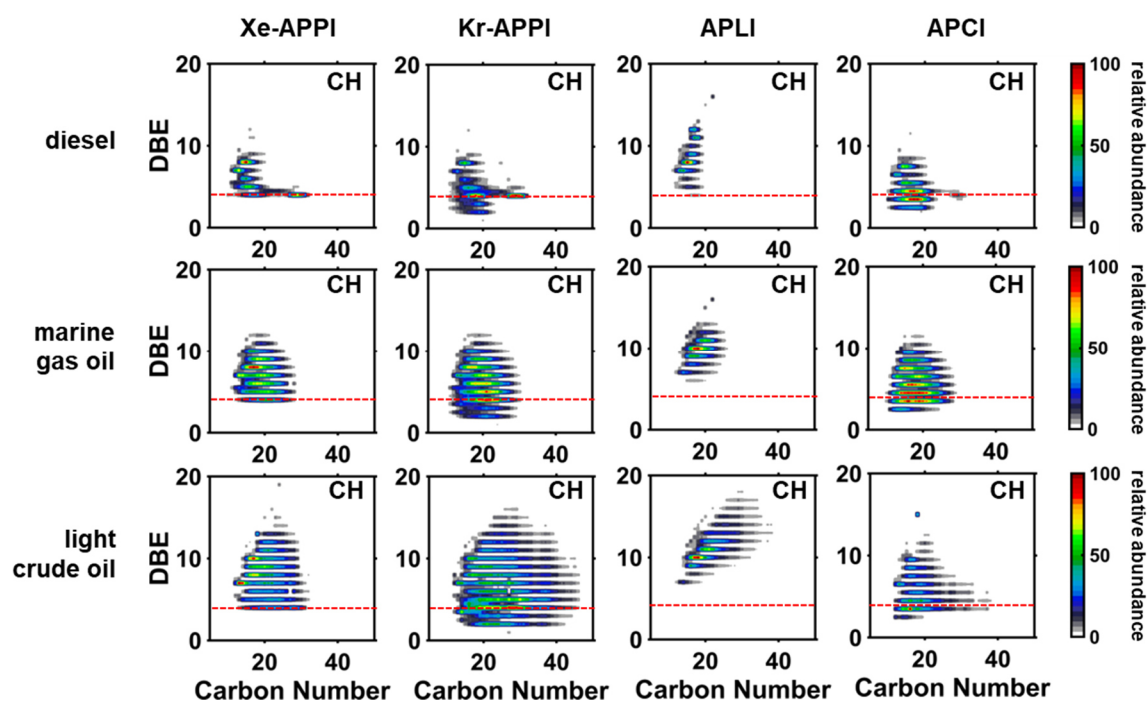


Figure 5. DBE vs. #C isoabundance diagrams of diesel, MGO, and light crude oil illustrate the compositional space covered by the different ionisation techniques. Radical cations and protonated ions are shown for the CH-class of all samples. The dashed red line at DBE 4 helps for orientation.

Detection of sterane biomarkers in complex mixtures

Although API techniques cover a broad range of chemical classes, pure alkanes can only be ionised under very specific conditions.⁵⁴ However, steranes and hopanes, which are tetracyclic respectively pentacyclic cycloalkanes, were shown to be ionisable by APPI^{27,55} and APCI.^{56–58} Steranes comprise the molecular skeleton of steroids, a group of biologically active compounds that also implies a variety of hormones⁵⁹ or neurotransmitters⁴⁰. As steroid compounds contain a variety of functional groups, double bonds or aromatic rings, it is not surprising that these compounds can be easily ionised by different API techniques.² However, as linear alkanes are typically not detected in API ionisation, we found it remarkable that we observed partially very high intensities for sterane-like cycloalkanes.

Sterane and hopane biomarkers are often used in literature to determine the maturity and origin of crude oil derived materials.⁶⁰ Juyal et al., for example, identified a high amount of hopanoic biomarkers in an unconventional crude oil by APPI-FT-ICR MS validated by GCxGC MS. In the present study, we investigated a diesel fuel that was surprisingly enriched in steranes compared to other commercially available fuels (Figure 6). For this sample, in Figure 6, the TICs are shown for all ionisation techniques. Furthermore, we added a spectrum

obtained by classical electron ionisation (EI) that was measured on an Agilent 7820 low resolution quadrupole GC-MS for direct comparison to standard GC-MS.⁶¹ The red highlighted area marks the retention time range in which steranes were detected. Kr-APPI reveals strikingly high response for steranes, although the standard GC-MS shows no signal in the respective time ranges. For the analysis of standard compounds, APCI and Xe-APPI showed only very weak signals for the sterane (Figure 1), whereas in the complex sample, steranes are clearly visible in the marked retention time range. APLI does not ionise any steranes as expected since lifetimes of the excited state of cycloalkanes⁶² are much lower than compared to aromatics.⁶³

For the very high TIC intensity of steranes in the Kr-APPI spectrum, one could assume that this effect is caused by the formation of both protonated ions and radical cations. However, it was found that steranes produce almost entirely radical molecular cations regardless the applied ionisation technique. In Figure S3, the direct comparison of the standard compound 5- α -cholestane mass spectra is shown for Xe-APPI and Kr-APPI. The molecular ion is in both cases the radical cation and protonated molecular ions were not detected. Fragment ions are very similar to those observed in literature.^{56,58,64} Figure S6 shows the averaged mass spectrum of the retention time range highlighted in red for Xe-APPI, Kr-APPI, and APCI. Also here, the precursor ions are present mostly as radical cations, whereas fragments presumably reveal hydride-abstracted ions that exhibit similarities to fragments observed by EI-MS.⁶⁵ APCI reveals the lowest intensity for sterane compounds but highest fragmentation. However, even APCI reveals predominantly radical cations for the sterane molecular ions which solidifies, on the one hand, that steranes are favourably ionised as radical cations, and gives, on the other hand, an explanation for the comparatively low intensity in APCI, since the mechanism of direct charge transfer is not very pronounced.^{57,66} Nonetheless, a study of Takahata et al. might present an explanation for the high ionisation efficiency of steranes in Kr-APPI.⁶⁷ The authors calculated the ionisation energies of 5 α -androstane that were revealed to be 10.60 eV and 10.67 eV for the two lowest ionisation energies, which match exactly with the photon energy of 10.6 eV provided by krypton discharge lamps. An explanation given for these two low ionisation energies is given by the electronic structure and long-range interactions of substituents in larger cycloalkanes.^{66,68}

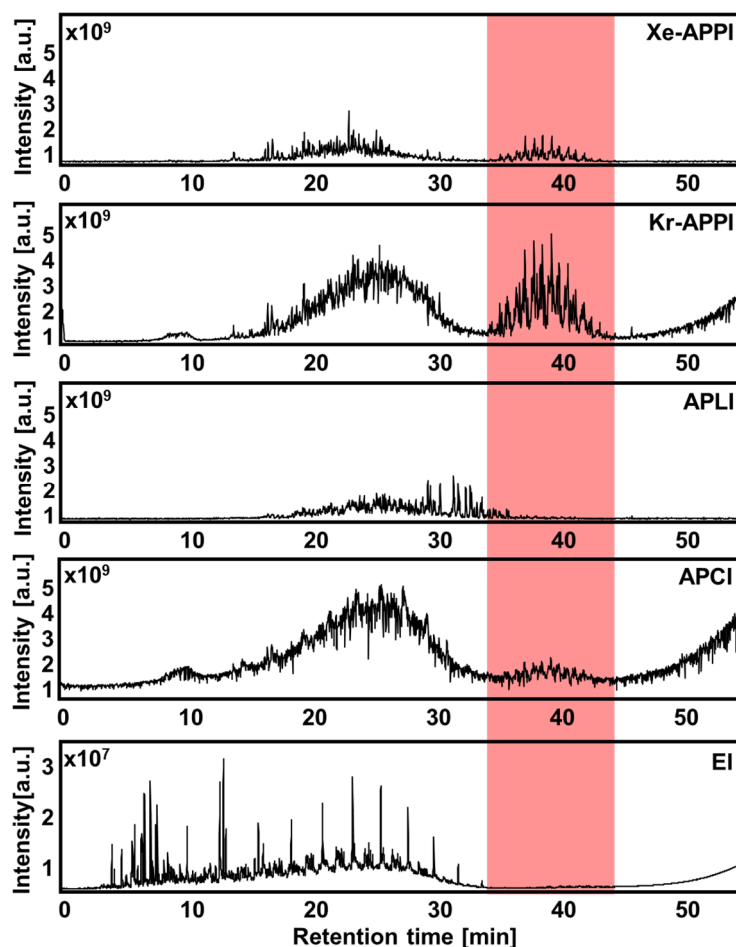


Figure 6. Total ion chromatogram (TIC) of an unconventional diesel fuel measured by GC-FTICR MS equipped with different API techniques. The bottom panel provides a GC-EI-Q-MS spectrum for direct comparison to classical GC-MS. The red highlighted retention time range marks the range in which sterane-type compounds were detected.

Distribution of radical cations and protonated ions

Compounds with integer and half-integer DBE were observed in complex mixtures for all ionisation techniques, however, the abundance strongly varies between the different methods. This effect was investigated in detail with four sequent exemplary light crude oil distillation cuts. The results are presented in Figure 7a as stacked bar plots for the different DBE values of the main compound classes. The ratio of radical cations (odd) and protonated ions (even) was calculated for each sample from intensity as well as number. Trends are summarised in Figure 7b for all compound classes and additionally in Table S4/S5 and Figure S7 for the individual CH-class and heteroatom-containing classes.

With increasing distillation temperature, the composition of the distillation cuts become more complex that includes an increase in the presence of heteroatoms (S, N, O), molecular mass, and aromaticity.⁶⁹ With regard to Figure 7, it was found that the odd/even ratio changes with the progression of distillation cut temperature. Xe-APPI and Kr-APPI show especially for lower distillation cuts, which are enriched in low-DBE value species, the formation of both ion types. Xe-APPI revealed an intensity-based odd/even ratio of 73:27 % for the lowest distillation cut, whereas Kr-APPI was more balanced with a ratio of 55:45 %. When the distillation cuts become more aromatic and complex, radical cations are preferentially formed. For Xe-APPI and Kr-APPI, the highest distillation cut (320-350 °C) reveals over 90 % and 80 % of radical cations, respectively. This trend becomes even more clear, when the odd/even ratios are plotted for the individual distillation cuts. For the intensity-based ratio, a strong increase of radical cations can be abstracted from Figure 7b for both APPI techniques. The number-based ratios show the same trend, but are less pronounced for Kr-APPI. Interestingly, when compounds are divided into the CH-class and heteroatom-containing classes (Figure S7), the number-based odd/even ratio stays relatively constant for the CH-class, but shows an increase for heteroatom-containing compounds. These observations point out a fluent transition to a more favoured direct photoionisation/radical cation formation for higher molecular weight/ higher aromatic compounds for gas phase sample introduction, whereas for the ionisation of non or low aromatic/ low molecular weight species, chemical reactions such as proton or charge transfer are more important. Interestingly, for liquid sample introduction, where solvents interact with the analytes, the contrary effect was noticed.³⁸

For APLI, the formation of protonated ions is uncommon with regard to the two-photon ionisation mechanism. Nevertheless, also ions with half-integer DBE values were found, which can, however, be attributed to hydride-abstracted molecular ions $[M-H]^+$. This type of fragmentation was also observed for standard substances discussed above. As the even ions are produced by fragmentation and not due to a chemical ionisation pathway, we did not show the odd/even ratio for APLI in Figure 7b.

In contrast to the other ionisation techniques, APCI is clearly dominated by more polar compounds and especially oxygen-containing species. Those polar to semi-polar compounds reveal especially high intensity (95-98 %) for protonated ions. The CH-class also shows high

abundant protonated ions, but also up to 10 % of the intensity was attributed to radical cations. For the number-based ratios, the differences were much smaller. CH-class compounds show an odd/even ratio of approximately 40:60, heteroatom-containing compounds of approximately 15:85. Interestingly, there was no trend observed neither for the intensity-based ratio, nor for the number-based ratio. Therefore, we can conclude that there is no favoured protonation or charge transfer mechanism for lower molecular weight/low aromatic or high molecular weight/high aromatic compounds as it was observed for the APPI-techniques.

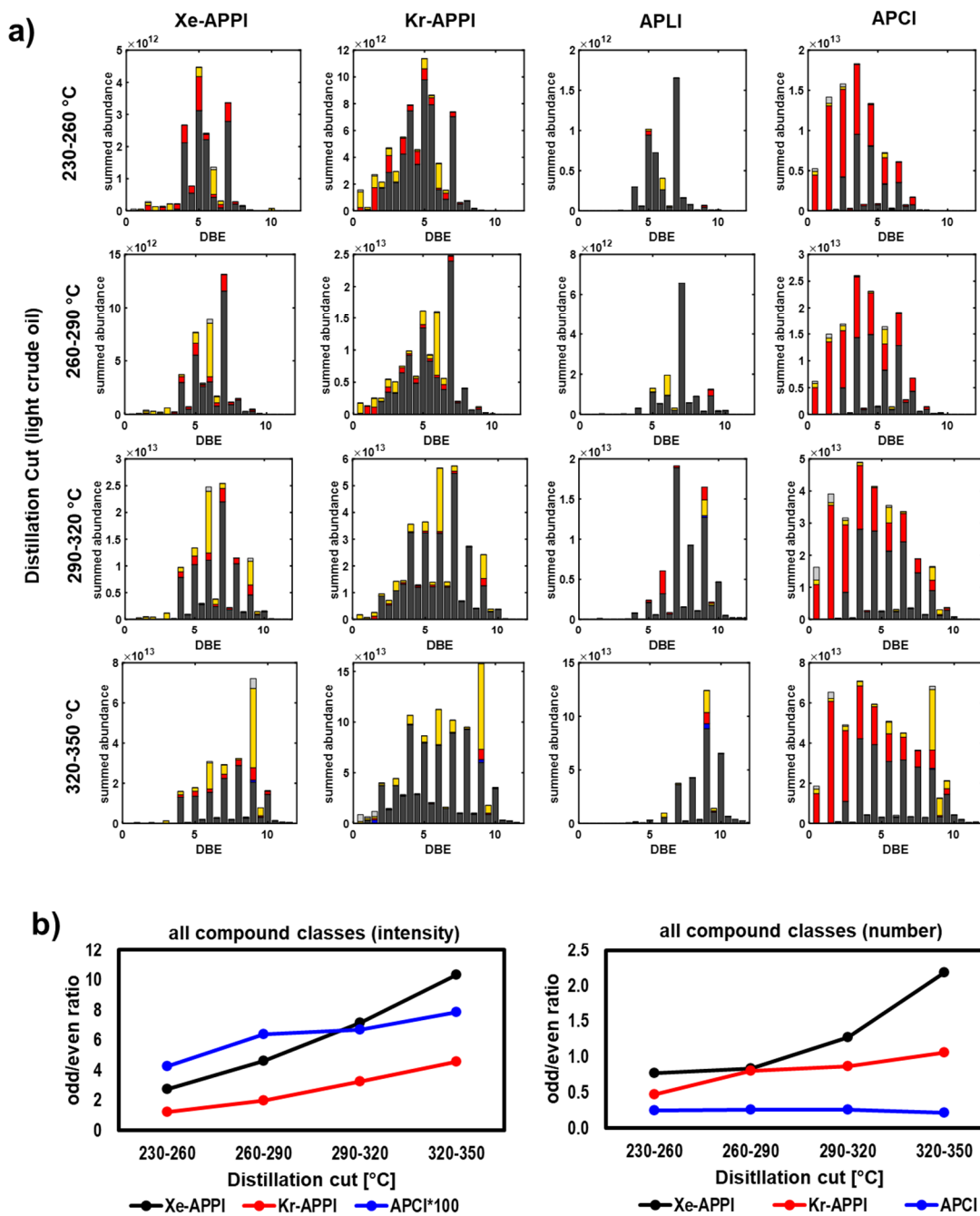


Figure 7. a) Stacked bar plots for the main compound classes for the covered DBE values range found in four sequent distillation cuts of a light crude oil. Xe-APPI, Kr-APPI and APCI show clear trends for the favoured ions formed in correlation with the DBE value. Compounds with low DBE values reveal high amounts of protonated ions, whereas for compounds with higher DBE values, the ionisation mechanism is more shifted towards the formation of radical cations. b) Ratio of radical cations (odd) and protonated ions (even) weighted by intensity and number for the different distillation cuts.

Conclusion

In this study, we examined the ionisation characteristics of a Xenon discharge lamp (Xe-APPI, 9.6/8.4 eV) for atmospheric pressure photoionisation. The results investigating a multicomponent standard composed of 45 different constituents as well as different complex petrochemical matrices are compared to established ionisation schemes, such as atmospheric pressure chemical ionisation (corona discharge plasma), atmospheric pressure photoionisation with a Krypton discharge lamp (Kr-APPI, 10.6/10 eV) and atmospheric pressure laser ionisation ([1+1], 2x4.7 eV, 266 nm). Hyphenation of gas chromatography to ultra-high resolution mass spectrometry (FT-ICR MS) allowed addressing the gas-phase ionisation behaviour without the usage of a dopant and in-depth chemical elucidation via sum formulae attribution and retention time separation.

For the multicomponent standard mixture, we observed ionisation of all contained PAHs by all ionisation techniques, regardless of the size of the aromatic core or the grade of alkylation, except of acenaphthylene not detected by APLI. However, thiol and ester compounds could not be detected by Xe-APPI and APLI. Protonated ions $[M+H]^+$ (even) could mass spectrometrically separated from the ^{13}C isotope of the radical cation $[M]^+•$ (odd), and the odd-to-even ratio was used as a descriptor for the ionisation behaviour. Interestingly, a high tendency to generate oxygenated artefact could be found for Xe-APPI. This finding can be explained by a VUV absorption band of oxygen at the emission wavelength of the Xenon discharge plasma (148 nm, 8.4 eV) and can certainly be considered a disadvantage. However, beneficially, almost no chemical background, commonly caused by APCI or Kr-APPI due to column bleed, plasticisers or impurities, is observed for Xe-APPI and APLI. This advantage is particularly helpful and important for evolved gas analysis without pre-separation or for chromatographic co-elution of complex mixtures. We conclude that this absence of chemical background noise can be of high interest for analysing samples with strong contamination.

Comparison of the attributed formulae of the different ionisation schemes via UpSet plots and fingerprint visualisation (DBE versus #C), revealed a rather limited and narrow chemical space ionised by Xe-APPI. Noteworthy, no unique CH-class compound could be attributed for investigating petroleum matrices, such as marine gas oil, by Xe-APPI compared to the other techniques. Xe-APPI especially addresses aromatic core structures (DBE 7-10) with lower alkylation (#C < 20) by prevalent direct photoionisation. However, both Xe-APPI and Kr-APPI

could sensitively detect sterane cycloalkanes, validated by gas chromatographic retention. Here, almost entirely radical molecular cations, regardless of the applied ionisation technique were found. Sterane and hopane biomarkers are often used in literature and Xe/Kr-APPI might offer new analytical workflows.

Future studies will further explore the ionisation characteristics of novel photoionisation schemes. Here, other discharge lamps, such as deuterium (continuous spectrum from 180-370 nm) and argon (11.7 eV, 106 nm), will be studied. Even gas mixtures, allowing the adjustment of the emission characteristics, could be used for tuning ionisation behaviour and selectivity. For this purpose, also state-of-the-art laser concepts can be deployed, such as wide-range optical parametric oscillators (OPO), studying wavelength-dependent ionisation responses.⁷⁰ For this upcoming research, the nature of the complex samples and related analytical standard constituents will be broadened, covering environmental samples, such as particulate matter extracts, or novel materials in energy transitions, such as bio- and recycling oils.

Acknowledgement

Funding by the Horizon 2020 program for the EU FT-ICR MS project (European Network of Fourier-Transform Ion-Cyclotron-Resonance Mass Spectrometry Centers, Grant agreement ID: 731077) is gratefully acknowledged. The authors thank the German Research Foundation (DFG) for funding of the Bruker FT-ICR MS (INST 264/56).

Declaration of Competing Interest

The authors report no declarations of interest. There are no conflicts to declare.

Associated Content

Supporting Information: The supporting information is available free of charge at XXX.

Compound list for the analytical standards (Table S1/S2); Average odd/even ratios for standards grouped into compound classes (Table S3); Intensity- and number-based odd/even ratios for the complex samples (Table S4/S5); Total intensities of selected compounds for all ionisation techniques (Figure S1); Odd/even ratios for selected compounds for APCI (Figure S2); Mass spectrum for 5 α -cholestane for Kr-APPI and Xe-APPI (Figure S3); Comparison of background signal of all ionization techniques (Figure S4); Comparison of Kr-APPI and Xe-APPI for complex sample thermal analysis with contamination (Figure S5); Summed mass spectra of the sterane-type compounds observed in diesel (Figure S6); intensity-and number-based odd/even ratio for all compounds as well as divided into the CH-class and heteroatom-containing classes (Figure S7).

References

- 1 F. W. McLafferty, *Annual review of analytical chemistry (Palo Alto, Calif.)*, 2011, **4**, 1–22.
- 2 T. J. Kauppila, J. A. Syage and T. Benter, *Mass spectrometry reviews*, 2017, **36**, 423–449.
- 3 a) A. Venter, M. Nefliu and R. Graham Cooks, *TrAC Trends in Analytical Chemistry*, 2008, **27**, 284–290; b) D. Freitas, X. Chen, H. Cheng, A. Davis, B. Fallon and X. Yan, *ChemPlusChem*, 2021, **86**, 434–445; c) R. M. Alberici, R. C. Simas, G. B. Sanvido, W. Romão, P. M. Lalli, M. Benassi, I. B. S. Cunha and M. N. Eberlin, *Analytical and bioanalytical chemistry*, 2010, **398**, 265–294;
- 4 D.-X. Li, L. Gan, A. Bronja and O. J. Schmitz, *Analytica chimica acta*, 2015, **891**, 43–61.
- 5 a) A. Raffaelli and A. Saba, *Mass spectrometry reviews*, 2003, **22**, 318–331; b) J. F. Ayala-Cabrera, L. Montero, S. W. Meckelmann, F. Uteschil and O. J. Schmitz, *Analytica chimica acta*, 2022, 340379;
- 6 J. F. Ayala-Cabrera, L. Montero, S. W. Meckelmann, F. Uteschil and O. J. Schmitz, *Analytica chimica acta*, 2022, 340353.
- 7 M. F. Mirabelli, J.-C. Wolf and R. Zenobi, *The Analyst*, 2017, **142**, 1909–1915.
- 8 J. F. Ayala-Cabrera, J. Turkowski, F. Uteschil and O. J. Schmitz, *Anal. Chem.*, 2022, **94**, 9595–9602.
- 9 J.-P. Hieta, R. Vesander, M. Sipilä, N. Sarnela and R. Kostianen, *Analytical chemistry*, 2021, **93**, 9309–9313, <https://pubs.acs.org/doi/pdf/10.1021/acs.analchem.1c01127>.
- 10 C. P. Rüger, A. Neumann, M. Sklorz and R. Zimmermann, *Anal. Chem.*, 2021, **93**, 3691–3697.
- 11 J. Pól, M. Strohal, V. Havlíček and M. Volný, *Histochemistry and cell biology*, 2010, **134**, 423–443.
- 12 J. A. Syage, M. A. Hanning-Lee and K. A. Hanold, *Field Analyt. Chem. Technol.*, 2000, **4**, 204–215.
- 13 L. C. Short, S.-S. Cai and J. A. Syage, *Journal of the American Society for Mass Spectrometry*, 2007, **18**, 589–599.
- 14 C. N. McEwen, *International Journal of Mass Spectrometry*, 2007, **259**, 57–64.
- 15 a) T. J. Kauppila and J. Syage, in *Photoionisation and photo-induced processes in mass spectrometry. Fundamentals and applications*, ed. R. Zimmermann and L. Hanley, Wiley, Weinheim, 2021, pp. 267–303; b) T. J. Kauppila, H. Kersten and T. Benter, *Journal of the American Society for Mass Spectrometry*, 2014, **25**, 1870–1881;
- 16 T. J. Kauppila, T. Kuuranne, E. C. Meurer, M. N. Eberlin, T. Kotiaho and R. Kostianen, *Anal. Chem.*, 2002, **74**, 5470–5479.
- 17 J. A. Syage, *Journal of the American Society for Mass Spectrometry*, 2004, **15**, 1521–1533.
- 18 S. Schmidt, M. F. Appel, R. M. Garnica, R. N. Schindler and T. Benter, *Analytical chemistry*, 1999, **71**, 3721–3729.
- 19 T. J. Kauppila, H. Kersten and T. Benter, *Journal of the American Society for Mass Spectrometry*, 2015, **26**, 1036–1045.
- 20 a) S. Große Brinkhaus, J. B. Thiäner and C. Achten, *Analytical and bioanalytical chemistry*, 2017, **409**, 2801–2812; b) R. Schiewek, R. Mönnikes, V. Wulf, S. Gäb, K. J. Brockmann, T. Benter and O. J. Schmitz, *Angewandte Chemie (International ed. in English)*, 2008, **47**, 9989–9992;

- 21 P. Benigni, J. D. DeBord, C. J. Thompson, P. Gardinali and F. Fernandez-Lima, *Energy Fuels*, 2016, **30**, 196–203.
- 22 R. Schiewek, M. Schellentträger, R. Mönnikes, M. Lorenz, R. Giese, K. J. Brockmann, S. Gäb, T. Benter and O. J. Schmitz, *Analytical chemistry*, 2007, **79**, 4135–4140.
- 23 H. Kersten, M. Lorenz, K. J. Brockmann and T. Benter, *Journal of the American Society for Mass Spectrometry*, 2011, **22**, 1063–1069.
- 24 I. Dzidic, D. I. Carroll, R. N. Stillwell and E. C. Horning, *Anal. Chem.*, 1976, **48**, 1763–1768.
- 25 R. Kostianen and T. J. Kauppila, *Journal of Chromatography A*, 2009, **1216**, 685–699.
- 26 M. J. Thomas, H. Y. H. Chan, D. C. Palacio Lozano and M. P. Barrow, *Anal. Chem.*, 2022, **94**, 4954–4960.
- 27 D. B. Robb, T. R. Covey and A. P. Bruins, *Anal. Chem.*, 2000, **72**, 3653–3659.
- 28 a) R. P. Rodgers, M. M. Mapolelo, W. K. Robbins, M. L. Chacón-Patiño, J. C. Putman, S. F. Niles, S. M. Rowland and A. G. Marshall, *Faraday discussions*, 2019, **218**, 29–51; b) J. L. Sterner, M. V. Johnston, G. R. Nicol and D. P. Ridge, *Journal of mass spectrometry : JMS*, 2000, **35**, 385–391; c) B. M. Ruddy, C. L. Hendrickson, R. P. Rodgers and A. G. Marshall, *Energy Fuels*, 2018, **32**, 2901–2907, <https://pubs.acs.org/doi/pdf/10.1021/acs.energyfuels.7b03204>; d) C. N. McEwen and R. G. McKay, *J. Am. Soc. Mass Spectrom.*, 2005, **16**, 1730–1738;
- 29 a) T. J. Kauppila, A. P. Bruins and R. Kostianen, *J. Am. Soc. Mass Spectrom.*, 2005, **16**, 1399–1407; b) J. S. de Wit and J. W. Jorgenson, *Journal of Chromatography A*, 1987, **411**, 201–212;
- 30 T. Schwemer, C. P. Rüger, M. Sklorz and R. Zimmermann, *Analytical chemistry*, 2015, **87**, 11957–11961.
- 31 a) M. P. Barrow, K. M. Peru and J. V. Headley, *Anal. Chem.*, 2014, **86**, 8281–8288; b) E. C. Horning, D. I. Carroll, I. Dzidic, S. Lin, R. N. Stillwell and J.-P. Thenot, *Journal of chromatography. A*, 1977, **142**, 481–495; c) I. A. Revelsky, Y. S. Yashin, T. G. Sobolevsky, A. I. Revelsky, B. Miller and V. Oriedo, *European journal of mass spectrometry (Chichester, England)*, 2003, **9**, 497–507;
- 32 M. Farenc, Y. E. Corilo, P. M. Lalli, E. Riches, R. P. Rodgers, C. Afonso and P. Giusti, *Energy Fuels*, 2016, **30**, 8896–8903.
- 33 a) A. G. Marshall and C. L. Hendrickson, *Annual review of analytical chemistry (Palo Alto, Calif.)*, 2008, **1**, 579–599; b) I. Jonathan Amster, *J. Mass Spectrom.*, 1996, **31**, 1325–1337;
- 34 A. G. Marshall and R. P. Rodgers, *Accounts of chemical research*, 2004, **37**, 53–59.
- 35 a) J. Hertzog, C. Mase, M. Hubert-Roux, C. Afonso, P. Giusti and C. Barrère-Mangote, *Energy Fuels*, 2021, **35**, 17979–18007; b) R. P. Rodgers and A. M. McKenna, *Analytical chemistry*, 2011, **83**, 4665–4687;
- 36 a) A. Gaspar, E. Zellermann, S. Lababidi, J. Reece and W. Schrader, *Analytical chemistry*, 2012, **84**, 5257–5267; b) C. Mase, M. Hubert-Roux, C. Afonso and P. Giusti, *Journal of Analytical and Applied Pyrolysis*, 2022, **167**, 105694; c) S. K. Panda, K.-J. Brockmann, T. Benter and W. Schrader, *Rapid communications in mass spectrometry : RCM*, 2011, **25**, 2317–2326; d) A. Kondyli and W. Schrader, *Rapid communications in mass spectrometry : RCM*, 2020, **34**, e8676;
- 37 J. Hertzog, V. Carré, Y. Le Brech, C. L. Mackay, A. Dufour, O. Mašek and F. Aubriet, *Analytica chimica acta*, 2017, **969**, 26–34.

- 38 A. K. Huba, K. Huba and P. R. Gardinali, *The Science of the total environment*, 2016, **568**, 1018–1025.
- 39 C. P. Rüger, T. Schwemer, M. Sklorz, P. B. O'Connor, M. P. Barrow and R. Zimmermann, *European journal of mass spectrometry (Chichester, England)*, 2017, **23**, 28–39.
- 40 T. J. Kauppila, T. Nikkola, R. A. Ketola and R. Kostianen, *Journal of mass spectrometry : JMS*, 2006, **41**, 781–789.
- 41 S. K. Panda, J. T. Andersson and W. Schrader, *Angewandte Chemie (International ed. in English)*, 2009, **48**, 1788–1791.
- 42 A. Li, T. Uchimura, H. Tsukatani and T. Imasaka, *Analytical sciences : the international journal of the Japan Society for Analytical Chemistry*, 2010, **26**, 841–846.
- 43 O. P. Haefliger and R. Zenobi, *Analytical chemistry*, 1998, **70**, 2660–2665.
- 44 P. Linstrom, *NIST Chemistry WebBook, NIST Standard Reference Database 69*, 1997.
- 45 P. Adam, B. Mycke, J. C. Schmid, J. Connan and P. Albrecht, *Energy Fuels*, 1992, **6**, 553–559.
- 46 H. Kersten, V. Funcke, M. Lorenz, K. J. Brockmann, T. Benter and R. O'Brien, *Journal of the American Society for Mass Spectrometry*, 2009, **20**, 1868–1880.
- 47 H.-C. Lu, H.-K. Chen, H.-F. Chen, B.-M. Cheng and J. F. Ogilvie, *A&A*, 2010, **520**, A19.
- 48 A. Neumann, M. L. Chacón-Patiño, R. P. Rodgers, C. P. Rüger and R. Zimmermann, *Energy Fuels*, 2021, **35**, 3808–3824.
- 49 C. P. Rüger, T. Miersch, T. Schwemer, M. Sklorz and R. Zimmermann, *Anal. Chem.*, 2015, **87**, 6493–6499.
- 50 J. Venn, *The London, Edinburgh, and Dublin Philosophical Magazine and Journal of Science*, 1880, **10**, 1–18, https://www.cis.upenn.edu/~bhusnur4/cit592_fall2014/venn%20diagrams.pdf.
- 51 a) O. O. Mofikoya, M. Mäkinen and J. Jänis, *Phytochemical analysis : PCA*, 2022, **33**, 392–401; b) A. Lex, N. Gehlenborg, H. Strobel, R. Vuillemot and H. Pfister, *IEEE transactions on visualization and computer graphics*, 2014, **20**, 1983–1992;
- 52 A. G. Marshall and R. P. Rodgers, *Proceedings of the National Academy of Sciences of the United States of America*, 2008, **105**, 18090–18095.
- 53 C. Gehm, T. Streibel, J. Passig and R. Zimmermann, *Applied Sciences*, 2018, **8**, 1617.
- 54 L. V. Tose, F. M. Cardoso, F. P. Fleming, M. A. Vicente, S. R. Silva, G. M. Aquije, B. G. Vaz and W. Romão, *Fuel*, 2015, **153**, 346–354.
- 55 P. Juyal, A. M. McKenna, A. Yen, R. P. Rodgers, C. M. Reddy, R. K. Nelson, A. B. Andrews, E. Atolia, S. J. Allenson, O. C. Mullins and A. G. Marshall, *Energy Fuels*, 2011, **25**, 172–182.
- 56 V. V. Lobodin, E. V. Maksimova and R. P. Rodgers, *Anal. Chem.*, 2016, **88**, 6914–6922.
- 57 L. M. Souza, L. V. Tose, F. M. R. Cardoso, F. P. Fleming, F. E. Pinto, R. M. Kuster, P. R. Filgueiras, B. G. Vaz and W. Romão, *Fuel*, 2018, **225**, 632–645.
- 58 C. Wu, K. Qian, C. C. Walters and A. Mennito, *International Journal of Mass Spectrometry*, 2015, **377**, 728–735.
- 59 a) A. Leinonen, T. Kuuranne and R. Kostianen, *Journal of mass spectrometry : JMS*, 2002, **37**, 693–698; b) M. J. Greig, B. Bolaños, T. Quenzer and J. M. R. Bylund, *Rapid communications in mass spectrometry : RCM*, 2003, **17**, 2763–2768;
- 60 a) W. K. Seifert and J. Michael Moldowan, *Geochimica et Cosmochimica Acta*, 1979, **43**, 111–126; b) C. Eiserbeck, R. K. Nelson, K. Grice, J. Curiale and C. M. Reddy, *Geochimica et*

- Cosmochimica Acta*, 2012, **87**, 299–322; c) J. J. Brocks and K. Grice, in *Encyclopedia of Geobiology*, ed. J. Reitner and V. Thiel, Scholars Portal, Dordrecht, 2011, pp. 147–167;
- 61 B. R. T. Simoneit, *Mass spectrometry reviews*, 2005, **24**, 719–765.
- 62 Y. Katsumura, Y. Tabata and S. Tagawa, *Radiation Physics and Chemistry (1977)*, 1982, **19**, 267–276.
- 63 S.-H. Lee, K.-C. Tang, I.-C. Chen, M. Schmitt, J. P. Shaffer, T. Schultz, J. G. Underwood, M. Z. Zgierski and A. Stolow, *J. Phys. Chem. A*, 2002, **106**, 8979–8991.
- 64 K. Hirota and R. Nakane, *Tetrahedron Letters*, 1968, **9**, 5909–5912.
- 65 a) B. J. Kimble, J. R. Maxwell, R. P. Philp and G. Eglinton, *Chemical Geology*, 1974, **14**, 173–198; b) L. Tokes, G. Jones and C. Djerassi, *J. Am. Chem. Soc.*, 1968, **90**, 5465–5477;
- 66 L. Pasa-Tolic, L. Klasinc, H. Spiegl, J. V. Knop and S. P. McGlynn, *Int. J. Quantum Chem.*, 1992, **41**, 815–827.
- 67 Y. Takahata and R. Vendrame, *Journal of Molecular Structure: THEOCHEM*, 1997, **391**, 169–178.
- 68 L. Klasinc, L. Tolić, H. Spiegl, J. V. Knop and S. P. McGlynn, *Computers & Chemistry*, 1990, **14**, 287–294.
- 69 a) M. M. Boduszynski, *Energy Fuels*, 1988, **2**, 597–613; b) A. M. McKenna, G. T. Blakney, F. Xian, P. B. Glaser, R. P. Rodgers and A. G. Marshall, *Energy Fuels*, 2010, **24**, 2939–2946; c) D. C. Podgorski, Y. E. Corilo, L. Nyadong, V. V. Lobodin, B. J. Bythell, W. K. Robbins, A. M. McKenna, A. G. Marshall and R. P. Rodgers, *Energy Fuels*, 2013, **27**, 1268–1276;
- 70 T. Streibel, K. Hafner, F. Mühlberger, T. Adam and R. Zimmermann, *Applied spectroscopy*, 2006, **60**, 72–79.